EXPERIMENTAL INVESTIGATION OF FREE AND IMPINGING SWIRLING TURBULENT JETS WITH DIFFERENT INFLOW CONDITIONS

Sergey V. Alekseenko, Artur V. Bilsky, Vladimir M. Dulin, Dmitriy M. Markovich
Institute of Thermophysics,
Siberian Branch of Russian Academy of Sciences
Ak. Lavrentyev ave. 1, Novosibirsk, 630090, Russia
aleks@itp.nsc.ru, bilsky@itp.nsc.ru, vmd@itp.nsc.ru, dmark@itp.nsc.ru

ABSTRACT

The local structure of swirling free and impinging turbulent jets is investigated experimentally under the following conditions: jet Reynolds number was equal to 8,900, the nozzle-to-plate distance was equal to three nozzle diameters and the swirl rate was varied from 0 to 1.0. Influence of the impinging plate on the flow structure is examined. It was demonstrated that separation bubble properties are rather sensitive to the presence of impinging wall. The effect of external periodical oscillations imposed on the inlet velocity was studied with various forcing amplitudes. The flow response to the forcing at two Strouhal numbers, St = 0.5 and 1.2, was examined. It was revealed, that for the swirling jet at S = 1.0, which so far was considered to be insensitive to the external forcing, the forcing at St = 1.2 with relatively high amplitude ($u'_0 > 5\%$ of the mean flow rate velocity) results an abrupt change in turbulent structure of the jet and leads to intensification of azimuthal large-scale fluctuations.

INTRODUCTION

Swirling jets are widespread in a variety of industrial applications: propulsion systems, such as jet engines, burners, etc. In combustion devices, one of the basic peculiarities of strongly swirling jets is a presence of reverse flow near the nozzle, which provides reliable stabilization of the flame. In chemical reactors and mixing chambers, faster spreading of the swirling jets relatively to the non-swirling ones, plays a major role and leads to a larger entrainment of surrounding media. A number of swirling flows is observed in nature (tornados, water spouts, etc.) which have to be carefully studied in order to forecast and prevent catastrophes.

The basic physics of swirling flows is presented in the monograph by Gupta et al. (1984). Introduction to a theory of helical vortices appearing in swirl flows can be found in Alekseenko et al. (1999). Detailed studies of different types of swirling flows were done in a number of works, considering different geometries and configurations. Swirling free jets were also investigated by different authors (Ribeiro and Whitelaw, 1980; Mehta et al., 1991; Billant et al., 1998; Loiseleux and Chomaz, 2003; Gallaire et al., 2004; Liang and Maxworthy, 2005; etc.). Most of these works are devoted to the analysis of azimuthal instabilities in the swirling jets and to the study of vortex breakdown at comparatively small Reynolds numbers (up to 1,000).

More interesting and less studied case from the practical and fundamental points of view is an impinging jet with superimposed swirl. There are only few works presenting experimental and numerical results on structure of swirling impinging jets (Owsenek et al., 1997; Huang and El-Genk, 1998; Nozaki et al., 2003; Abrantes and Azevedo, 2006). In these works the impinging heat transfer was studied for a variety of flow parameters, particularly, swirl rate and nozzle-to-plate distance. Presently, experimental data on hydrodynamic structure of swirling impinging jet flows is restricted by distributions of the mean velocity and intensities of velocity fluctuations.

An external low-amplitude forcing of inlet velocity can be a key to control turbulent mixing in the initial region of swirling jets, similarly to the non-swirling ones (Crow and Champagne, 1971; Zaman and Hussain, 1981). The effect of forcing of the free swirling jets at various frequencies and azimuthal modes was investigated in the works by Panda and McLaughlin (1994) and Gallaire et al. (2004). For flow conditions preceding the vortex breakdown, these studies showed that axisymmetric or azimuthal forcing intensifies development of corresponding instabilities and leads to domination of axisymmetric or helical vortices, respectively. For swirling jets with high swirl rates, Gallaire et al. (2004) have shown that the vortex breakdown appears to be insensitive to the forcing attempts, at least for the studied parameters.

Generally, on the basis of previous works, it can be underlined that combined application of swirl and external forcing can be used for the enhancement of mixing in chemical reactors, burners and mixing devices utilizing confined jets configurations.

From the other hand, for development and validation of developing computational fluid dynamics (CFD) codes it is also necessary to provide comprehensive experimental data, in particular, on turbulent swirling free and impinging jets because they contain specific zones traditionally arduous for modeling (shear layers, stagnation point, vortex breakdown, number of spiral-type instabilities, etc.).

Particle Image Velocimetry gives an additional opportunity to obtain the spatial distributions of instantaneous flow velocity and, consequently, direct measurement of the spatial velocity derivatives, terms of dissipation rate, spatial spectra, two-point correlations, etc. However, for correct estimation of the above-mentioned quantities, it is necessary to elaborate a number of complex pre- and post-processing PIV algorithms.

The objective of the present work is an experimental study of the hydrodynamic structure of free and impinging turbulent jets with swirl. The main emphasis was done on the analysis of influence of near-placed solid surface and of external forcing on the structure of the swirling jet flow.

EXPERIMENTAL SETUP, APPARATUS AND DATA PROCESSING

The experimental setup represented a hydrodynamic loop equipped with a pump, a flowmeter and a temperature stabilizing device. Water flow was driven by pump which rotation speed was precisely controlled by an inverter. A thermostat was used to maintain a constant water temperature of 26 °C with an accuracy of ±0.2 °C. The measurements were

performed in a rectangular working section (40 cm height, 20 cm width, 20 cm length) made of plexiglas in order to provide PIV measurements. The Reynolds number, defined on the basis of the mean flow rate velocity $U_0 = 5.2$ m/s and nozzle diameter $d = 15$ mm, was equal to 8,900. Both free and impinging swirling jets were studied. In the latter case, an impingement surface was mounted normally to the flow at the distance of $H/d = 3$ from the nozzle exit (Figure 1b). During the experiments, the swirl rate S was varied from 0 to 1.0. For swirl organization, smoothing grids in a plenum chamber of the nozzle were replaced by a swirl generator. The definition of a swirl number (1), following to Gupta et al. (1984), was based on geometrical parameters:

$$S = \frac{2}{3}\left(\frac{1-\left(d_1/d_2\right)^3}{1-\left(d_1/d_2\right)^2}\right)\tan(\varphi) \qquad (1)$$

Here, $d_1 = 7$ mm is the diameter of a centerbody supporting the blades, $d_2 = 27$ mm is the external diameter of the swirler, and φ is the blade inclination angle.

External periodical perturbations were imposed on the flow by means of an exciter connected to a diaphragm. The diaphragm was mounted to a bottom of a mixing chamber connected to the nozzle plenum chamber by a pipe of one meter length. Amplitude of sine voltage supplying the exciter was controlled by a power amplifier. Two values of forcing frequency, corresponding to Strouhal number of St = 0.5 and 1.2 were examined.

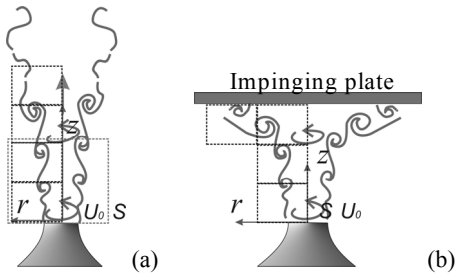

Figure 1: Schemes of (a) free and (b) impinging swirling jets and measurement areas location

The "PIV-IT" Stereo PIV system was used for the measurements. The system consisted of a double cavity Nd:YAG pulsed laser, couple of CCD cameras and a synchronizing processor. During the experiments, the system was operated by a computer with "ActualFlow" software. A laser sheet formed by set of cylindrical and focusing lenses. Depending on the measurement area size, polyamide particles with different mean diameters (10 or 20 μm) were used for flow seeding. The measurements were performed in a meridional plane (r, z) passing through the jet axis.

At the first stage, swirling free and impinging jets were studied without external forcing. In this case, in order to provide high spatial resolution, the whole measurement area was separated into elementary zones where the measurements were performed independently. The schemes of the studied flows and the measurement zones locations are shown in Figure 1a and b. For each zone, 3,000 image pairs were captured by each camera. The angle between the optical axis of each camera and the measurement plane normal was of 26°.

At the second stage, influence of the external forcing on the structure of free swirling jets was studied. In this case, for the whole flow field study, the measurement area was two times larger than in the first case and covered initial region of the jet (see Figure 1a).

All measured images were processed by an iterative cross-correlation algorithm with an image deformation and with a final interrogation area size of 32×32 pixels and 50% overlap. Calculated instantaneous velocity fields were then validated, "outliers" were removed, and the "holes" were interpolated before stereo reconstruction. A plane calibration target was employed for stereo calibration and a 3rd-order polynomial transform was used to minimize non-linear optical distortions. Additionally, an iterative correction of the laser and target plane misalignment was performed to improve the calibration quality. Instantaneous velocity derivatives were calculated from 3C velocity fields by using a second-order centered difference scheme.

RESULTS AND DISCUSSION

In this section of the work spatial distributions of statistical moments and examples of instantaneous velocity for the free and impinging swirling jets are presented. The studied jets have a general axial symmetry, and thus are described using a cylindrical coordinate system. Here, coordinates (r, θ, z) denote the radial, azimuthal and axial directions respectively. Correspondingly, (V, W, U) and (υ, w, u) are the radial, azimuthal and axial components of the mean and fluctuating velocity.

Free and impinging swirling jets

In the present subsection the influence of the impinging plate on the swirling jet structure is considered. In Figure 2 spatial distributions of the axial mean velocity are presented. For the impinging jet at the low swirl rate, $S = 0.41$, the lengthy recirculation zone characterized by a negative value of the axial mean velocity is observed unlike for the free jet. The recirculation zone develops directly from the impinging plate towards the nozzle exit and the axial velocity at the jet centerline maintains an almost constant small negative value in the range of $z/d = 0.5 – 2.5$. A similar behavior was reported by Nozaki et al. (2003) for the swirling impinging jet at Re = 4,000, $H/d = 2$ and $S = 0.43$. For the swirling jets at relatively high swirl rate, $S = 1.0$, the size of the recirculation zone is smaller than for impinging jet at S = 0.41, and a minimum of the axial velocity is located near the nozzle exit. Generally, the recirculation zone is found to be more pronounced in case of the impinging flow.

Figure 3 demonstrates spatial distributions of the axial component of the turbulent kinetic energy (TKE) for the jets. In general, for the whole presented area of the jets at $S = 0$ and $S = 1.0$, the value of $\langle u^2 \rangle$ (and actually all components of TKE, which are not presented) is higher for the case of impinging swirling jet. The highest values of TKE were found in the mixing layer developing from the edge of the nozzle ($S = 0$ and $S = 0.41$) and in the area close to the recirculation zone near the nozzle exit.

External forcing

In this subsection the application of external forcing to the free swirling jets is considered. The forcing was applied with two non-dimensional frequencies (Strouhal numbers): St = 0.5 and 1.2. These values of St were selected on the basis of preliminary calculated one-dimensional spatial spectra (not shown in the paper). For the mixing layer of the jets at $S = 0$ and 0.41, a clear spectrum peak was observed at low wavenumbers corresponding to St ≈ 0.5, which is close to natural frequency bandwidth of a jet 'column' (St = 0.3-0.5). For

$S = 1.0$, more pronounced peak at $St \approx 1.2$ was found for the spectra calculated along the mixing layer and across the recirculation zone. Various forcing amplitudes were considered by controlling power supplying the exciter. Average intensities u'_0 of the axial velocity fluctuations at the nozzle exit of the non-swirling jet are used as reference to forcing amplitude. The intensities were averaged over the following range of r/d: from -0.4 to 0.4, where their distribution was almost constant. Without forcing, u'_0/U_0 was found to be 0.033. During the forcing the highest reached values were 0.27 and 0.1 for the frequencies St = 0.5 and 1.2, respectively.

Figures 4-6 show distributions of the radial and axial components of TKE for the forced jets. It was found that the forcing has a minor effect on the mean velocity, and therefore its distributions are not presented. For the jets at $S = 0$ and 0.41, the forcing at St = 0.5 caused significant increase both of $\langle u^2 \rangle$ and $\langle \upsilon^2 \rangle$, while $\langle w^2 \rangle$ increased slightly (see a, b, c, e, f, and g cases in Figures 4, 5). The flow response to St = 1.2 forcing was found to be less pronounced (see d, and h cases in Figures 4, 5).

Otherwise, for the highly swirling jet (i.e. $S = 1.0$), forcing at St = 0.5 did not lead to significant changes in TKE magnitudes (Figure 6b and c) and only a moderate decrease of the recirculation zone longitudinal size was observed (not shown in the paper). When for $S = 1.0$ case the forcing was applied at St = 1.2, its effect on TKE was found to be substantial. For forcing amplitudes below 0.042, $\langle w^2 \rangle$ grows in some degree, while $\langle u^2 \rangle$ and $\langle \upsilon^2 \rangle$ remain almost unchanged (cf. Figure 6a, c, e and g). When the amplitude value is $u'_0/U_0 \geq 0.051$, the flow changes abruptly: $\langle u^2 \rangle$ and $\langle \upsilon^2 \rangle$ decrease and $\langle w^2 \rangle$ becomes great, as well as the total TKE.

To analyze the revealed effect, in Figure 7 the spatial distributions of instantaneous velocity fields are presented. Azimuthal components of velocity (Figures 7 d-e) and vorticity (Figures 7 a-c) are shown as contour maps. In case of the unforced jet with the low swirl $S = 0.41$ (Figure 7a, d), there is no recirculation zone observed, and asymmetric helical vortices developing near the jet centerline and in the outer mixing layer can be seen. For the high swirl rate $S = 1.0$, both forced ($u'_0/U_0 = 0.051$) and unforced cases are presented. The reverse flow near the jet axis is observed, and intense helical vortices are present in the inner and outer mixing layers. In the forced case the vortices seem to be less pronounced and to have a smaller size. More significant difference is observed in distributions of instantaneous azimuthal velocity w^* plotted in Figures 7e and f. While for the unforced jet, the azimuthal velocity is mainly positive to the left of the jet axis and negative to the right, large regions of w^* having opposite values are observed for the forced case. The presence of these large-scale energy-containing structures can be the reason of large values of $\langle w^2 \rangle$ observed for the forced cases with $u'_0/U_0 \geq 0.051$.

CONCLUSIONS

The turbulent structure of free and impinging swirling turbulent jets at Re = 8,900 and $S = 0$-1.0 is investigated experimentally by using Stereo PIV. It is demonstrated that the impinging plate significantly affects the whole swirling flow up to the nozzle exit and that its greatest influence is on the flow with relatively low swirl rate, $S = 0.41$. In this case a large recirculation zone appears which is not observed for the free jet. Also, it was shown that magnitudes of the turbulent kinetic energy components are rather higher in case of the impinging flow.

Analyzing swirling jets response to an external forcing, it was shown that for both non-swirling jet and jet with $S = 0.41$, the forcing at St = 0.5 leads to increase of turbulent kinetic energy generation with forcing amplitude, while for St = 1.2 this effect is significantly lesser. Contrary, for the jet at high swirl rate $S = 1.0$, forcing at St = 0.5 seems to give minor effect on the jet structure. Different behavior was revealed for the forcing at St = 1.2. At relatively high amplitude ($u'_0 > 5\%$ of the mean flow rate velocity) an abrupt change of turbulent structure of the jet was observed: large-scale contr-rotating structures appeared in the jet and while the azimuthal kinetic energy component increased significantly, the radial and axial components diminish in some degree.

ACKNOWLEDGEMENTS

This work is supported by RAS and SB RAS integration research projects and by the RFBR foundation, grant N 07-08-00213.

REFERENCES

Abrantes, J.K., and Azevedo, L.F.A, 2006, "Fluid Flow Characteristics of a Swirl Jet Impinging on a Flat Plate", Proceedings, 13th International Symposium on Application of Laser Techniques to Fluid Mechanics, Lisbon, Portugal, June 26-29, 2006.

Alekseenko, S.V., Kuibin, P.A., Okulov, V.L., and Shtork, S.I., 1999, "Helical Vortices in Swirl Flow" Journal of Fluid Mechanics, Vol. 382, pp. 195-243.

Billant, P., Chomaz, J.-C., and Huerre, P., 1998, "Experimental Study of Vortex Breakdown in Swirling Jets", Journal of Fluid Mechanics, Vol. 376, pp. 183-219.

Crow, S.C., and Champagne, F.H., 1971, "Orderly Structure in Jet Turbulence", Journal of Fluid Mechanics, Vol. 48, pp. 547-591

Gupta, A.K., Lilley, D.G., and Syred, N., 1984, "Swirl Flows", Abacus Press, Kent Engl.

Heinz, 0., Ilyushin, B., and Markovich, D., 2004, "Application of a PDF Based Method for the Statistical Processing of Experimental data", Int. Journal of Heat and Fluid Flow, Vol. 25, pp. 864-874.

Huang, L., and El-Genk, M.S., 1998, "Heat Transfer and Flow Visualization Experiments of Swirling, Multi-Channel, and Conventional Impinging jets", Int. Journal of Heat and Mass Transfer, Vol. 41, pp. 583-600.

Liang H., and Maxworthy T., 2005, "An Experimental Investigation of Swirling Jets", Journal of Fluid Mechanics, Vol. 525, pp. 115–159.

Loiseleux, T., and Chomaz, J.M., 2003, "Breaking of Rotational Symmetry in a Swirling Jet Experiment", Physics of Fluids, Vol. 15, pp. 511-523.

Mehta, R.D., Wood, D.H., and Clausen P.D., 1991, "Some Effects of Swirl on Turbulent Mixing Layer Development", Physics of Fluids A, Vol. 3, pp. 2716-2724.

Nozaki, A., Igarashi, Y., and Hishida, K., 2003, "Heat Transfer Mechanism of a Swirling Impinging Jet in a Stagnation Region", Heat Transfer – Asian Research, Vol. 32(8), pp. 663-673.

Owsenek, B.L., Cziesla, T., Mitra, N.K., and Biswas, G., 1997, "Numerical Investigation of Heat and Mass Transfer in Impinging Axial and Radial Jets with Superimposed Swirl", Int. Journal of Heat Mass Transfer, Vol. 40, pp. 141-147.

Panda, J., and McLaughlin, D.K., 1994, "Experiments on the Instabilities of a Swirling Jet", Physics of Fluids, Vol. 6, pp. 263-276.

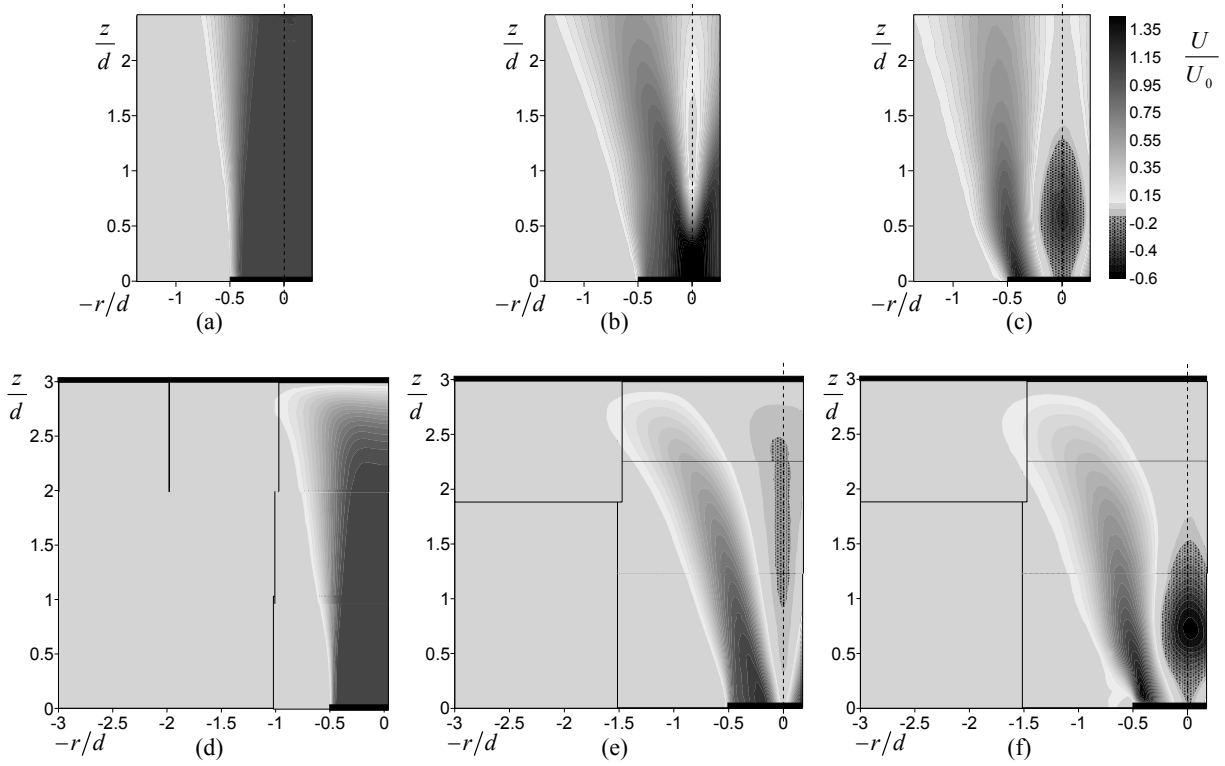

Figure 2: Spatial distributions of the axial mean velocity for the unforced jets. Free jets: (a) $S = 0$; (b) $S = 0.41$; (c) $S = 1.0$. Impinging jets: (a) $S = 0$; (b) $S = 0.41$; (c) $S = 1.0$

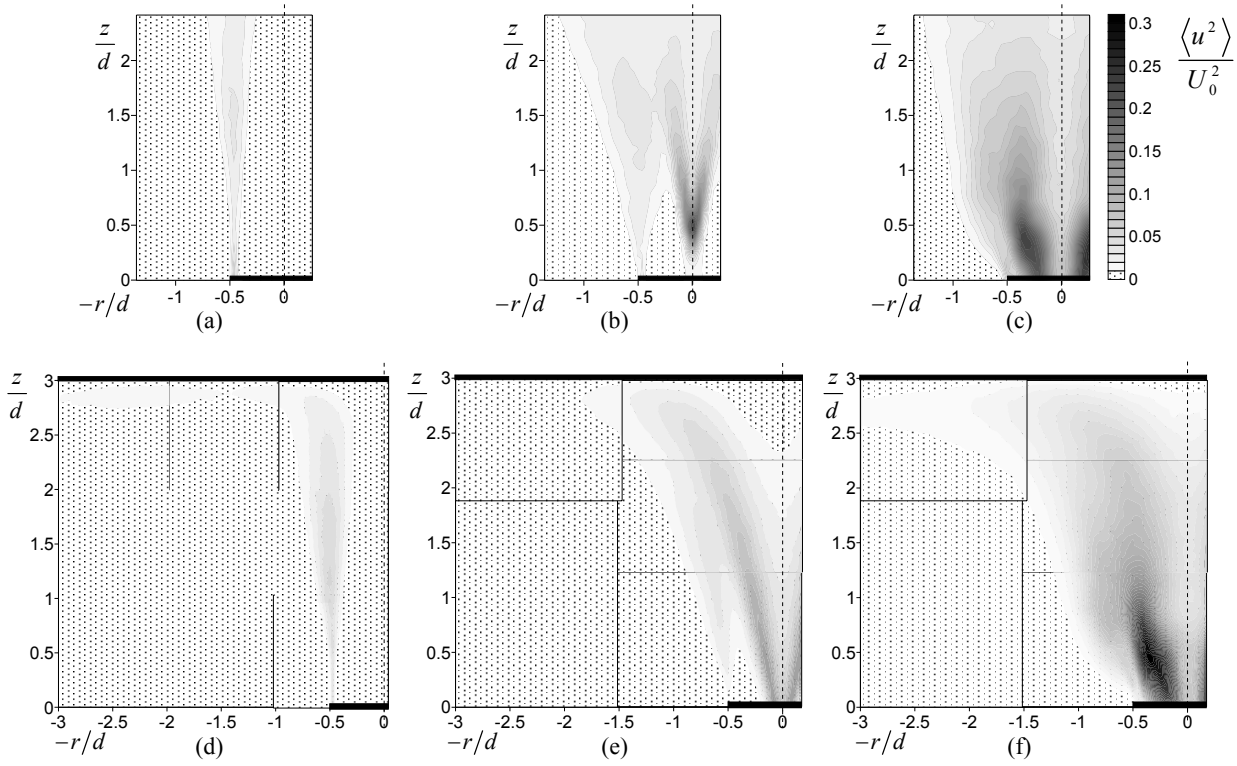

Figure 3: Spatial distributions of the axial component of TKE for the unforced jets. Free jets: (a) $S = 0$; (b) $S = 0.41$; (c) $S = 1.0$. Impinging jets: (a) $S = 0$; (b) $S = 0.41$; (c) $S = 1.0$

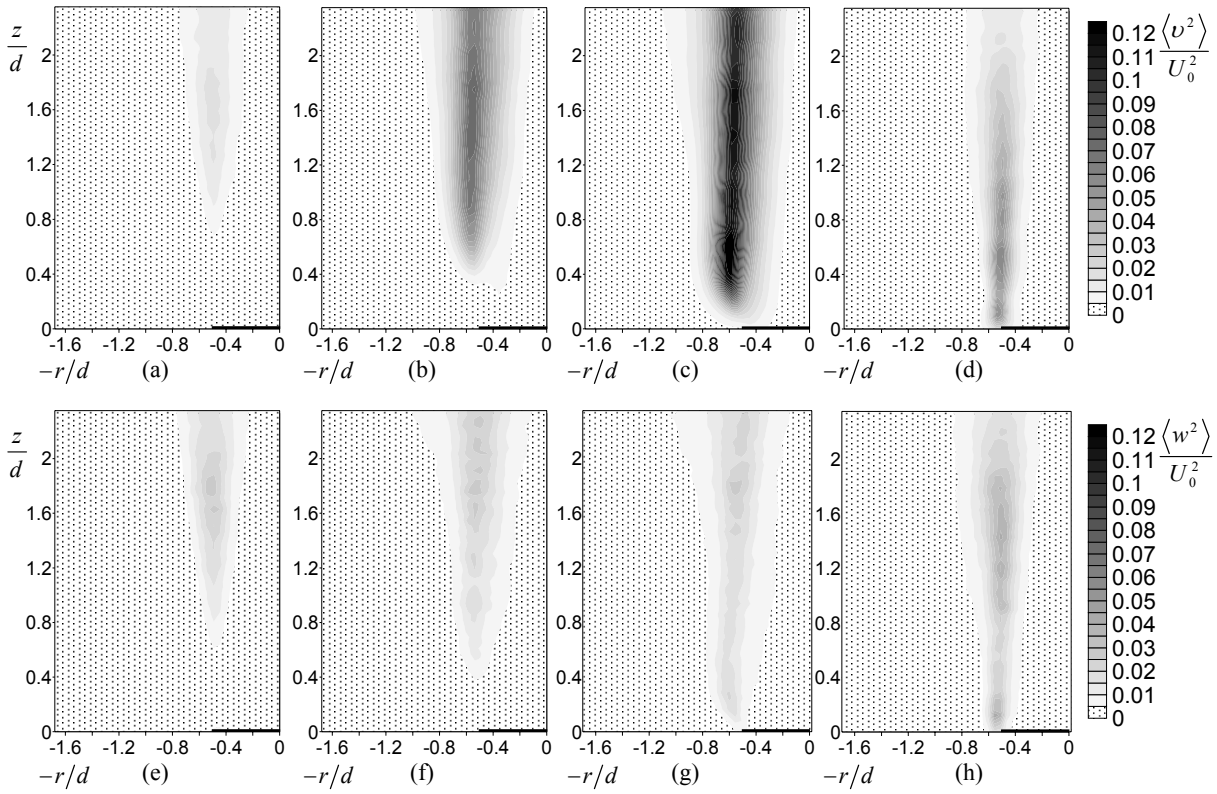

Figure 4: Radial and azimuthal components of TKE for free jet at $S = 0$. (a), (e): St = 0; (b), (f): St = 0.5, $u'_0/U_0 = 0.063$; (c), (g): St = 0.5, $u'_0/U_0 = 0.15$; (c), (g): St = 1.2, $u'_0/U_0 = 0.069$

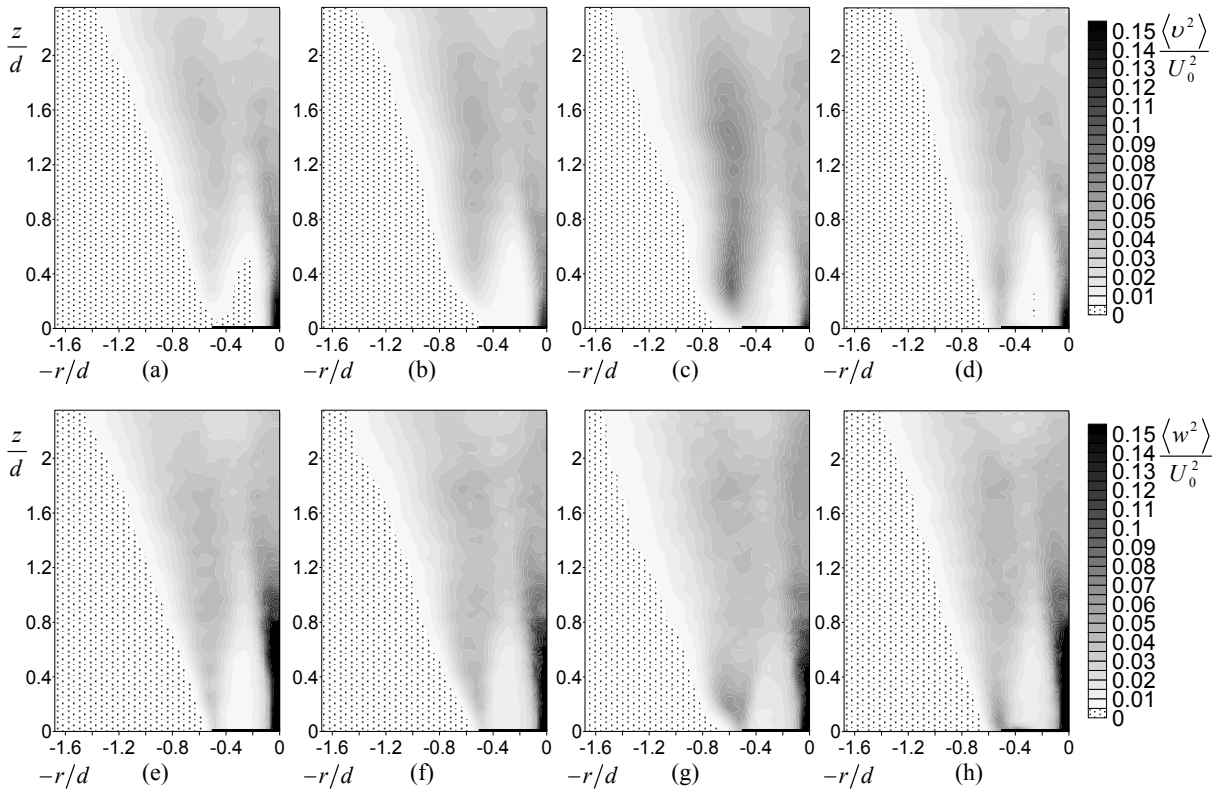

Figure 5: Radial and azimuthal components of TKE for free jet at $S = 0.41$. (a), (e): St = 0; (b), (f): St = 0.5, $u'_0/U_0 = 0.063$; (c), (g): St = 0.5, $u'_0/U_0 = 0.15$; (c), (g): St = 1.2, $u'_0/U_0 = 0.069$

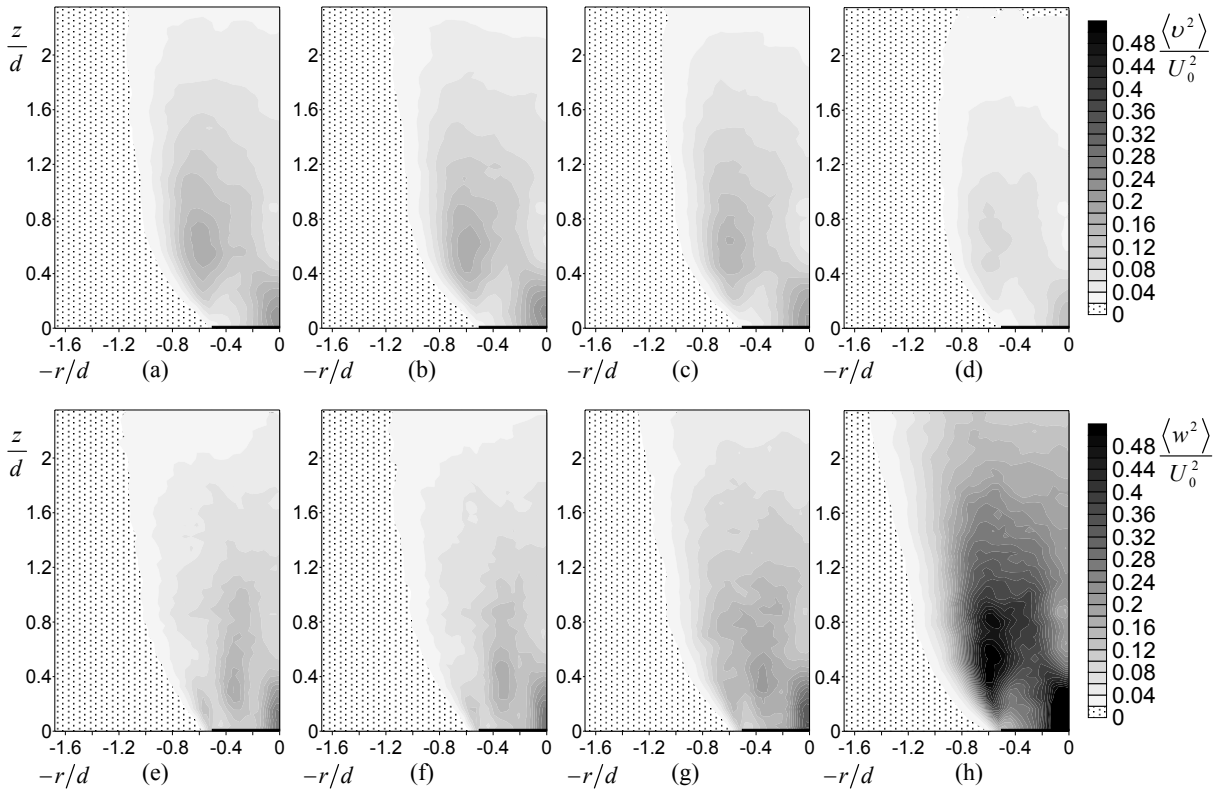

Figure 6: Radial and azimuthal components of TKE for free jet at $S = 1.0$. (a), (e): St = 0; (b), (f): St = 0.5, $u'_0/U_0 = 0.063$; (c), (g): St = 1.2, $u'_0/U_0 = 0.042$; (c), (g): St = 1.2, $u'_0/U_0 = 0.0051$

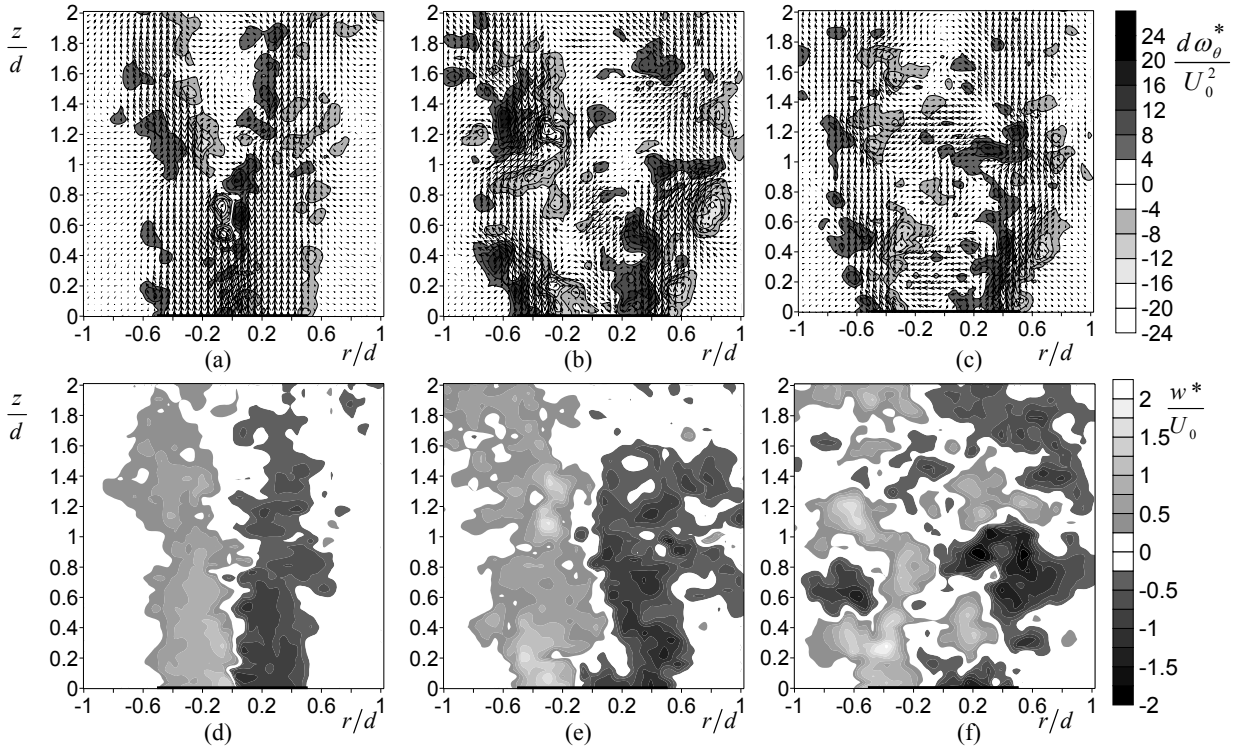

Figure 7: Instantaneous velocity and vorticity fields for the free swirling jets. (a), (d) $S = 0.41$, St = 0; (b), (e) $S = 1.0$, St = 0; (c), (f) $S = 1.0$, St = 1.2, $u'_0/U_0 = 0.051$